

Controlling self-assembly of engineered peptides on graphite by rational mutation

*Christopher R. So, Yuhei Hayamizu, Hilal Yazici, Carolyn Gresswell,
Dmitriy Khatayevich, Candan Tamerler, and Mehmet Sarikaya**

*Corresponding author: sarikaya@u.washington.edu

Supporting Information Contents

Supplementary Methods S1-S12	S1-S15
Supplementary Figures 1-5	S16-S20
References	S21

S1. Supplementary Methods: Combinatorial selection of graphite binding peptides by phage display

The Ph.D-12 phage display library (Fig S1A(i)), based on a combinatorial library of random 12-mer peptides fused to the minor coat protein(pIII) of M13 phage (New England BioLabs), was used to select peptide sequences against graphite powder (crystalline, ~300 mesh, 99%, 10129, Alfa Aesar) (Fig S1A(ii)). The 12-mer phage display library has an estimated diversity of 2.7×10^9 different random clones. To enrich the graphite binding clones, four selection rounds were carried out in the panning experiment (Fig. S1A). Prior to exposing powders to the phage library, graphite was cleaned by exposure to increasingly polar solvents in the presence of ultrasonication first in a methanol/acetone mixture, then in isopropanol, and lastly in DI water. The graphite powder was then dried under vacuum. 10 mg of graphite powder was exposed to a volume of 10 μ L of phage display library and incubated in potassium phosphate/sodium carbonate buffer (PC, 55 mM KH_2PO_4 , 45 mM Na_2CO_3 and 200 mM NaCl, pH 7.4), containing 0.1% detergent (combination of 20% (w/v) tween 20 and 20% (w/v) tween 80) for 30 min. on a rotator at room temperature and then washed twice before overnight incubation. Following overnight incubation, to remove the nonspecifically- or weakly-bound phage, the graphite powder was then washed (Fig S1A(iii)) ten times using PC buffer with increasing detergent concentrations from 0.1% to 0.5% (v/v), at pH: 7.2. The bound phage were then eluted (Fig S1A(iv)) from the surface in a stepwise manner by applying an elution buffer consisting of 0.2 M Glycine-HCl pH 2.2 (Sigma Aldrich, St. Louis, MO) for 15 min. Eluted phage were then transferred to an early log phase E. coli ER2738 culture (~OD: 0.5) and amplified for 4.5h (Fig. S1A(v)). The amplified phage were isolated by polyethylene glycol (PEG) precipitation (1,2). Purification of phage includes three main PEG-NaCl (20 % (w/v) PEG-8000 (Sigma) and 2.5 M NaCl (Sigma)) steps followed by re-suspension of phage precipitate in PC buffer with decreased volume. In the first step, 1:6 ratio PEG-NaCl (~40 mL) was added into supernatant that is recovered after centrifugation of E.coli and incubated overnight at 40C to precipitate phage. Following, phage pellet was obtained by centrifugation and re-suspended in 5 mL

PC. In the second and third steps, the same procedure was followed with decreased incubation times (2 hours and 10 min) and PC buffer volume (1 mL and 200 μ L). In the subsequent three selection rounds, graphite powder was exposed to the phage obtained from each previous round to enrich the phage pool in favor of the strongest-binding clones (Fig. S1A(vi)). Following the four rounds of panning, amino acid sequences of the

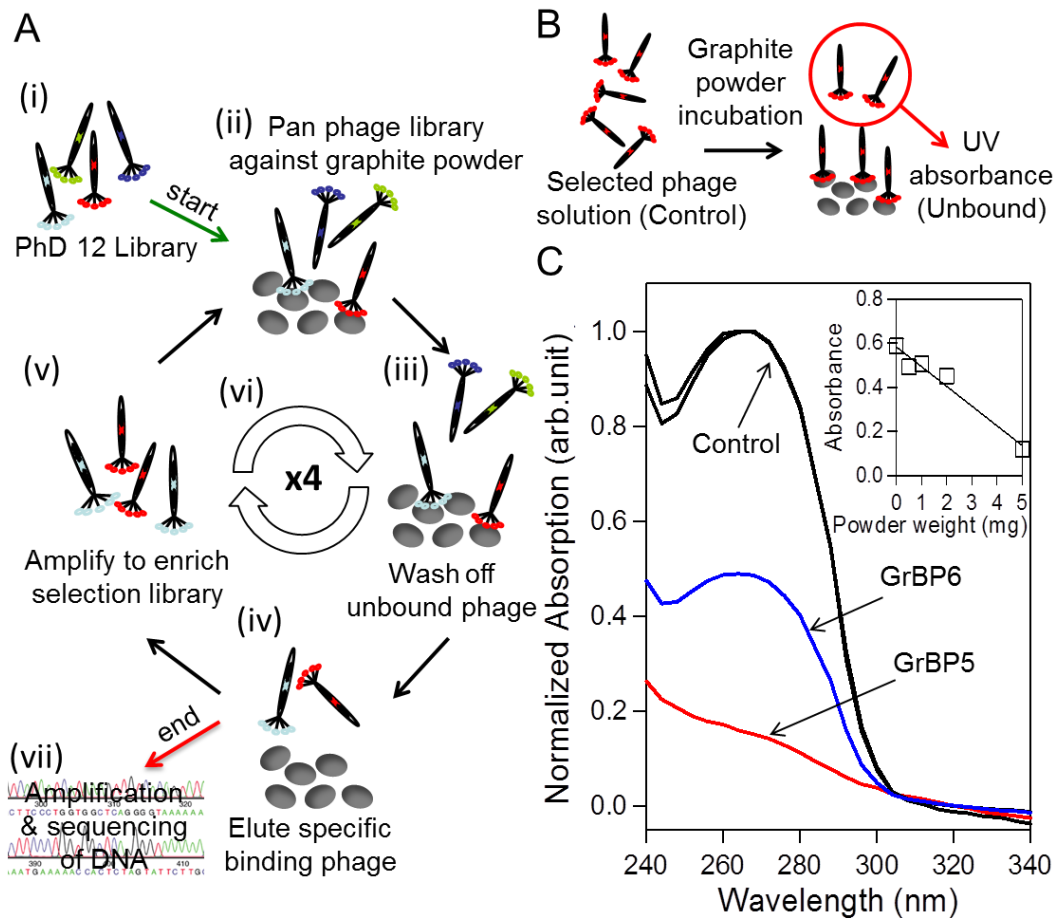


Figure S1. Graphite binding peptide selection and characterization methods: (A) Schematic representing phage display selection of graphite binding peptides by using the PhD 12 library for 4 rounds of biopanning. (B) Scheme for characterizing selected graphite binding clones and their affinity for graphite powder as quantified by spectrophotometry of circled unbound phage (depletion). (C) Normalized optical absorption spectra of clones shown according to the UV absorption of GrBP5 (strongest graphite binder, red) and GrBP6 (weakest graphite binder, blue) upon incubation with graphite powder and each solution before exposure (negative controls, black). Inset showing optimization of powder weight, where graphite powders from 0.5 mg, 1.0 mg, 2.0 mg to 5.0 mg all exist in a linear regime.

60 phage selected clones were amplified and identified by DNA sequencing (Fig. S1A(vii)). The single-stranded DNA of selected phage plaques were isolated by a QIAprep Spin M13 Kit (Qiagen, Valencia, CA) and amplified via PCR in the presence of dye-labeled terminators (Big dye terminator v3.1, Applied Biosystems, Carlsbad, CA). PCR products were purified by Shephadex G-50 column precipitation. A 96 gIII primer or 5'-OH CCC TC TAGTTA GCG TAA CG-3' primer was used for the amplification of ssDNA. The selected sequences of DNA from clones were analyzed by an Applied Biosystems 310 Avant genetic analyzer.

S2. Supplementary Methods: Characterization of graphite binding affinity by spectrophotometric quantification of phage

The selected clones, following sequencing, were then tested individually for their binding affinities. To measure clone binding affinity, we adopted spectrophotometry (3) to quantify both the amplified phage starting solutions as well as their depletion due to reaction with graphite powder (Fig. S1B). Phage concentrations in the range 10^{10} - 10^{12} pfu/ml can be accurately determined by analyzing the broad optical absorption peak located from 260 nm to 280 nm, with a slight maximum at 269 nm (Fig. S1C). Since this peak reflects the nucleotide content of the particular phage, a molar extinction coefficient ($9.006 \times 10^3 \text{ M}^{-1} \text{ cm}^{-1}$) has been previously derived (3). This treatment was modified to reflect the genome size of M13KE used in our study, 7222 bp, as calculated below.

$$\text{Phage particles / ml} = \frac{(\text{Measured } A_{269} - \text{Measured } A_{320}) * (6 * 10^{16})}{7222 \text{ (The number of nucleotides in phage genome)}}$$

To quantify the relative binding strength of all selected clones, both phage concentration and powder weight were optimized to maximize the absorbance change upon phage reaction with graphite. First, a phage working concentration was found by forming an optimization curve (via absorbance of 10^{10} , 10^{11} and 10^{12} pfu/ml phage solutions) and choosing the greatest value from the linear regime, 10^{12} pfu/mL. Next, analogously, graphite powders of incremental weights (0.5, 1.0, 2.0 and 5.0 mg) were each exposed to 10^{12} pfu/ml phage solution to form a second optimization curve (inset of Fig. S1C),

establishing a working powder weight of 5 mg. Using these conditions, all selected clones were individually exposed to 5 mg of graphite powder in PC buffer and incubated for 24 hours on a rotator at room temperature to allow phage-inorganic powder surface interactions to occur. After incubation, the reacted graphite powder was pelleted by centrifugation at 5,000 rpm for 3 min and the supernatant (unbound phage) was used for spectrophotometric measurements. Relative binding affinities were calculated from the measured absorption intensities of depleted (unbound) phage solutions as a percentage of the original absorption intensity from starting solutions. Each experimental set was performed in triplicates and repeated twice, including a positive control of only 10^{12} pfu/ml selected phage clones with no graphite powder and a negative control that has no random insertion sequence (M13KO7 purchased from NEB, N0315S). Finally, the graphite binding peptides (GrBPs) were categorized and grouped as strong, moderate and weak binders (Fig. S2).

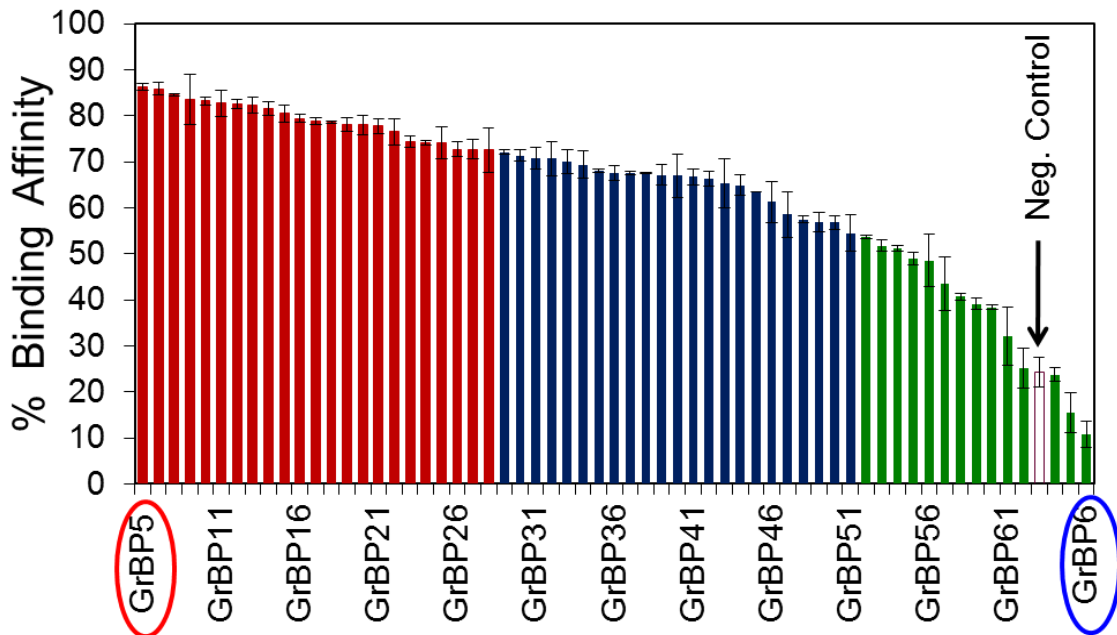


Figure S2. Binding affinity of selected phage clones characterized by photospectroscopy, in percentage, and their categorization in three binding groups: strong (in red), moderate (in blue) and weak binders (in green) versus negative control (M13KE) (in white).

S3. Supplementary Methods: Verification of clone affinity by Atomic Force Microscopy (AFM)

The strongest (GrBP5: IMVETESSDYSSY) and weakest (GrBP6: THPLPIHANELT) selected binders were verified quantitatively via AFM imaging and Langmuir modeling on highly ordered pyrolytic graphite (HOPG). Peptide sequences were synthesized and characterized for their affinity by drop coating HOPG samples with various concentrations of peptide for three hours. Samples were then scanned with high resolution tapping force AFM and coverage was quantified to form curves seen in Fig. S3. From this analysis, GrBP5 was found to have an equilibrium constant (K_{eq}) of $2.23 \mu\text{M}^{-1}$, which was about five-fold greater than $0.43 \mu\text{M}^{-1}$ K_{eq} of GrBP6. Interestingly, while GrBP6 contains His residues that may be involved with graphite binding, it lacks the cooperative interactions of GrBP5 that forms more highly covered ordered surfaces. The hydrophilic central region of GrBP5 may be related to the evolution of the three domains of GrBP5 from the phage screening process. It is likely that the central hydrophilic region of the peptide (IMVTESSDYSSY) allows a higher chance for selection, since soluble phages are preferable in the aqueous screening media. The other two domains, (IMVTESSDYSSY), contain amino acids which have been implicated in the literature to be associative towards graphite [aromatic (Wang, S. Q. et al., Nat. Mater. 2, 196-200, 2003), hydrophobic (Kowalewski, T. et. al., Proc. Natl. Acad. Sci., 96, 3688-3693, 1999)].

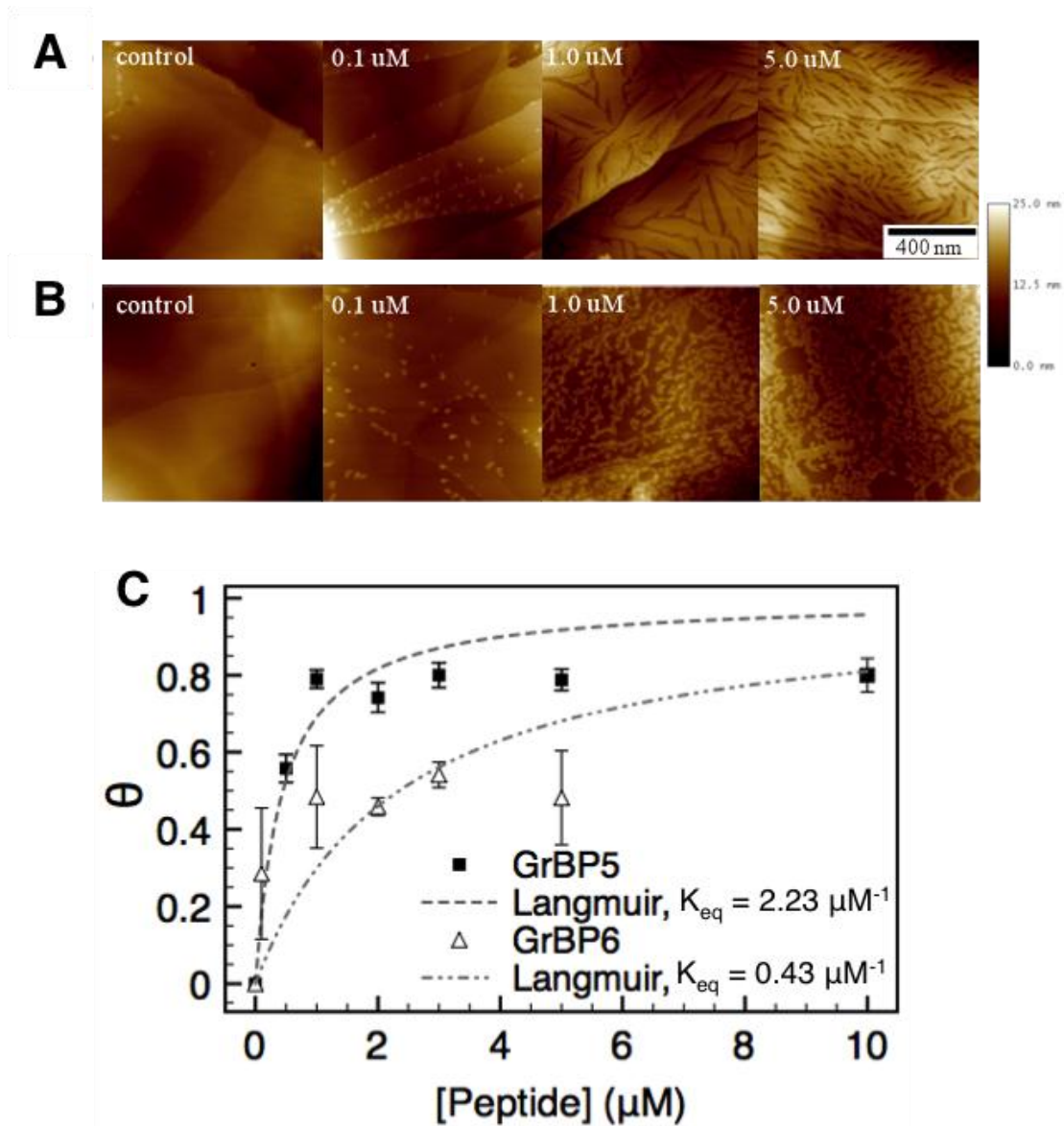


Figure S3. Characterization of strongest and weakest GrBPs on HOPG A) Representative images from control, 0.1, 1.0 and 5.0 μM GrBP5 solutions exposed to HOPG for three hours B) for GrBP6 and C) Quantification of surface coverage for GrBP5 and 6 with least square fitting from Langmuir modeling, revealing K_{eq} values displayed in legend.

S4. Supplementary Methods: Coverage of disordered vs. ordered peptides

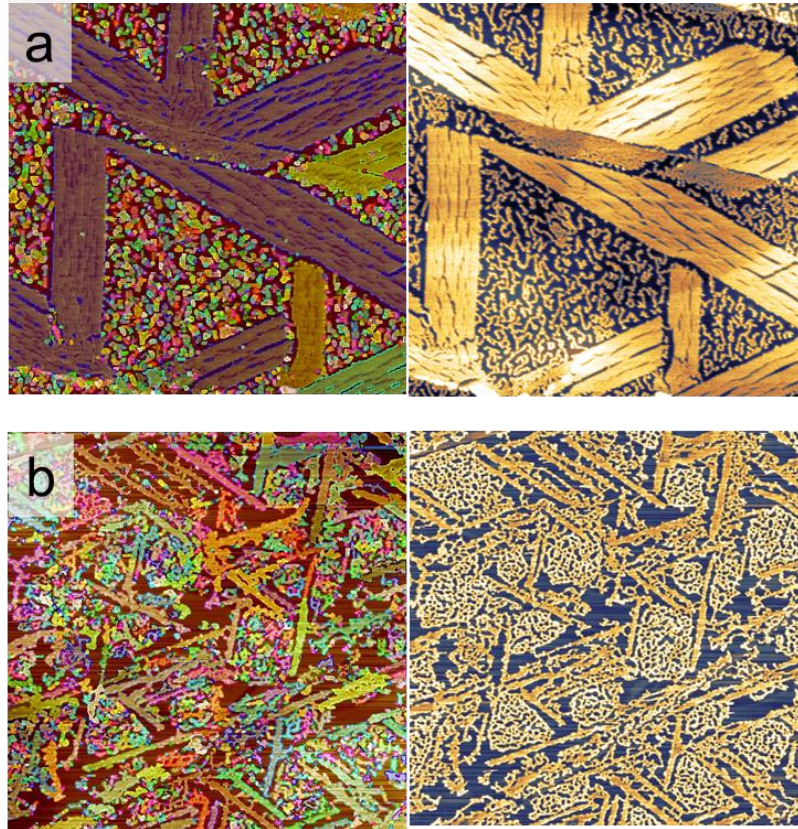


Figure S4. Mixed AP and OP images which were quantified for their contribution to total surface coverage as plotted in Fig. 2e. Colors distinguish particles based on a watershed segmentation tool which is sensitive to surface topography.

S5. Supplementary Methods: AFM data analysis and image processing

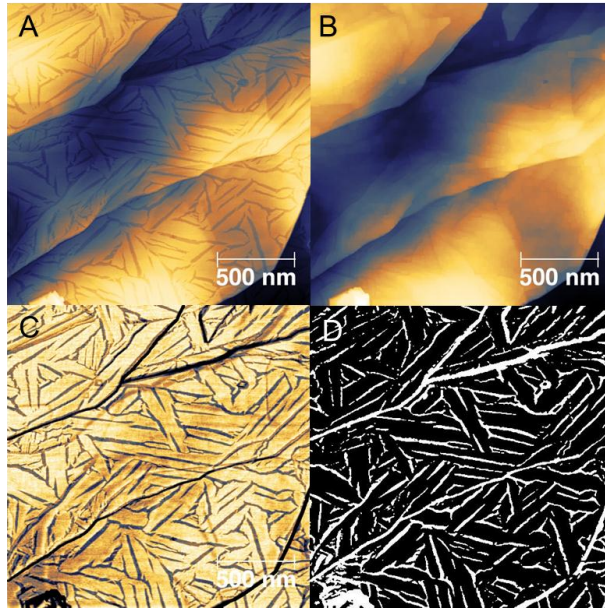


Figure S5. Image processing method for background subtraction: (A) Original AFM image of GrBP5 on HOPG, showing characteristic ‘waviness’ on a $3 \times 3 \mu\text{m}$ scan which prevents the definition of a planar threshold. (B) A dilation filter applied with a 6×6 pixel neighborhood to remove pores created by the peptide film, leaving (C): Original AFM image (B) subtracted from image (A), showing only peptide film morphology and the underlying HOPG. (D) Final binary counting mask of the original image (A) counting only the peptide film with normalized surface topography.

S6. Supplementary Methods: Peptide Height Measurements

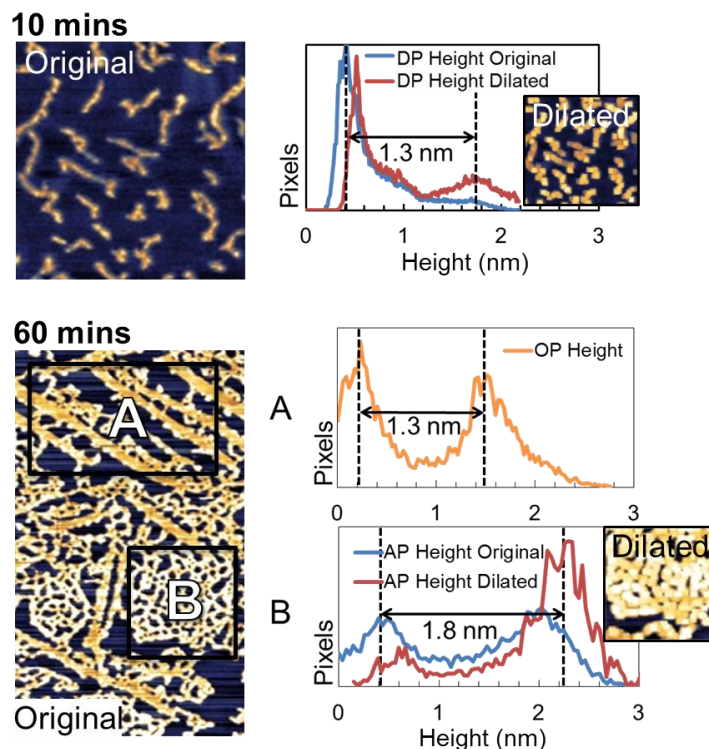


Figure S6. Method for measuring discretely bound peptide height across entire images. Plot shows both original (blue) and dilated (red) image histograms where bare surface is most accurate in blue and peptide height is most accurate in red. Peak corresponding to max peptide height is enhanced by image dilation. Average height is taken as the difference between these values. Same technique was used for images with both phases present, where height is taken independently from each phase.

S7. Supplementary Methods: Quantification of Deposition Rate D

The deposition rate of peptides onto the surface is defined by the relation: $D(t) = s * F(t)$

Where $D(t)$ is the deposition rate, s is the sticking coefficient of the peptide, and $F(t)$ is the flux rate of peptides hitting the surface, resulting from their bulk diffusion in solution. Since peptides used in this study are chemically similar, their size and hydrodynamic properties should result in similar $F(t)$ trends. Therefore, measuring $D(t)$ should directly

reflect their surface affinity from varied s values of different peptide sequences. The adsorption probability s is also a measure of peptide lifetime on the surface, including both binding and unbinding events. To quantify peptide arrival rates over time in our study, coverage values at 10 mins were divided by assuming a peptide surface area of 3.14 nm^2 with a radius of roughly 1 nm, established by molecular simulations to be detailed elsewhere. Coverage values were measured over ten separate $1 \text{ }\mu\text{m}^2$ regions on the surface using the methods outlined previously. Counts were then calculated as per second intervals. Errors in the main text were derived by taking the error in coverage from Figure 3d by the area of peptides, as was done to calculate the F value.

S8. Supplementary Methods: Quantification of Particle Density Change over Time

The change in number density of particles over time was determined by quantifying the number of features in each image over time. Methods described previously were used to measure the population of particles, defined as isolated features on the surface, over a combined minimum scanning area of $16 \text{ }\mu\text{m}^2$ (3-4 $2 \text{ }\mu\text{m} \times 2 \text{ }\mu\text{m}$ AFM images). For WT-GrBP5, images at 1 hour were already interconnected so earlier adsorption times, below 10 mins, shown in Supplementary Fig. 3, were required for measurable coarsening rates. Rates were measured from the linear region of the two curves in Supplementary Fig. 3, which was up to ~900 secs. for WT-GrBP5 and 10800 secs. for Mutant 2.

S9. Supplementary Methods: Determining Peptide Binding Affinity (K) on HOPG by AFM

WT GrBP5 and its five mutants were assessed for affinity towards HOPG by exposing surfaces to 0.5, 1.0 and 5.0 μM concentrations of 50 μL of each peptide for 3 hours. After three hours, samples were immediately flash frozen in a -80°C freezer (observed to take ~10 seconds) and freeze-dried using the protocol described in the M&M section of the main text. The results are shown in Supplementary Figure 4, where surface coverage quantification (described in Supplementary Methods S5) yields exponential behaviors

which can be modeled and quantified by fitting to an adsorption model for an affinity constant K .

To extract K values, the binding affinities of peptides to graphite were estimated from a relationship between the observed surface coverage of peptides by AFM and the peptide concentrations used for incubation. Here, we employed a simple adsorption equation based on reference 4 which allows us to approximate the binding affinity.

$$\theta = \theta_{max} \times \frac{K \times C}{1 + K \times C} \quad [1]$$

θ is coverage of peptides, θ_{max} is maximal coverage of peptides, C is concentration of peptide solution, and K is binding affinity constant.

S10. Supplementary Methods: Peptide Synthesis

As in our previous work, synthesis was carried out on a preloaded support resin using HBTU activation chemistry, while 20% piperidine in DMF was employed to afford the Fmoc deprotection and monitored by UV absorbance at 301 nm. Following solid-phase synthesis, the peptides were cleaved off the support and side chain deprotected by stirring the resin-bound peptide in a cocktail (containing either 87.5:5:5:2.5

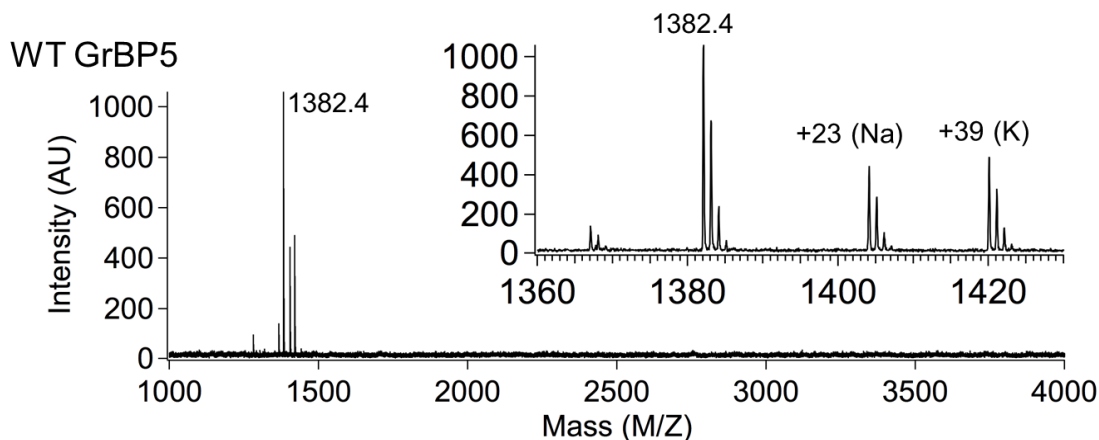


Figure S7. Representative MALDI Mass spectrum of GrBP5 showing purified peptide peak and peptide-ion adducts with Sodium (+23) and Potassium (+39) from synthesis glassware

TFA/thioanisole/H₂O/phenol/ethanedithiol or 94:1:2.5:2.5
TFA/triisopropylsilane/H₂O/EDT, depending on the peptide) under N₂ atmosphere for 2-3 hrs. The resin was removed by filtration, and each of the peptides was precipitated with cold ether to yield crude peptide product that was lyophilized (Virtis Benchtop K, SP Industries, Inc., Warminster, PA). Peptides were reconstituted using various ratios of DI H₂O and acetonitrile. Purification by reverse-phase HPLC for peptides employed, first, an isocratic (0% B for 2 min) and, then, a linear gradient of 1%/min for analytical and 0.5%/min for semiprep scales at 1 and 10 mL/min flow rates, respectively. Retention times spanned 30-50 mins depending on the peptide in semi-preparative HPLC. Analytical peaks were isolated by autothreshold collection (Waters Deltaprep 600, analytical mode) and peptides were verified by MALDI-TOF mass spectrometry with reflectron (RETOF-MS) on an Autoflex II (Bruker Daltonics, Billerica, MA) mass spectrometer in positive-ion mode. The observed M/Z fractions were subsequently collected manually from a scaled semi-preparative separation (Waters Deltaprep 600, semiprep. mode). The verified and collected masses and specific retention times are displayed in Table S1 and Fig. S7.

Peptide	Sequence	Theoretical Mass (MW)	Purified Mass (M/Z)	Shift	Retention Time (min.)
GrBP5-WT	IMVTESSDYSSY	1381.4	1382.4	+1(H)	34.88 , 1%/min, start 10%B
Mutant 1	IMVTESSDASSA	1197.2	1220.2	+22.8 (Na)	29.15 , slow 1%/3min, start 10%B
Mutant 2	IMVTESSDWSSW	1427.5	1428.65	+1 (H)	50.64, 1%/min
Mutant 3	IMVTESSDFSSF	1349.4	1388.54	+39 (K)	54.45 , 1%/min
Mutant 4	LIATESSDYSSY	1335.3	1335.4	0.1	53.90, 1%/min
Mutant 5	TQSTESSDYSSY	1354.3	1355.71	+1 (H)	41.5, 1%/min

Table S1. Table showing list of sequences used in this study with their theoretical mass and resulting purified mass as verified by MALDI-TOF MS subsequently used for experiments. Shifts from expected values are explained by trace elements picked up during the synthesis and purification processes (ie, Na and K from glassware). Retention times and deviations from the standard isocratic gradient are described that resulted in difference in time on the column.

S11. Supplementary Methods: Pendant drop analysis of peptide solutions

Pendant drop shape analysis, used to determine the liquid-air interfacial tension of solutions, relies on the distortion, by gravity, of a drop suspended from a syringe needle of a known diameter. By using the Young-Laplace equation interfacial tension is derived from the total volume of the drop, its vertical size, contact angle with the needle, and liquid density. In this case all of the geometric parameters were automatically obtained from the drop images using vendor-provided software (First Ten Angstroms, Inc, Portsmouth, VA) and the density of the liquid is assumed to be that of water. The results indicate no statistically significant differences in the interfacial tensions of various peptide solutions used in our experiments. See Fig S8.

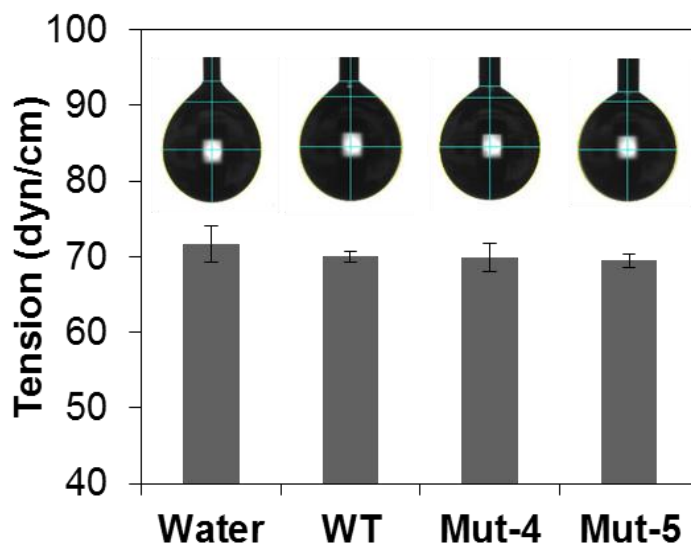


Figure S8. Air-liquid tensions of 1 μ M peptide solution pendant drops used during CA experiments. Calculated from the vendor-provided drop-shape analysis software using the Young-Laplace equation. Images of each respective pendant drop are displayed above each bar, showing similar drop shapes as measured by software represented by yellow outlines.

S12. Supplementary Methods: Size-exclusion chromatography of GrBP5

Solution state of GrBP5 was characterized by size-exclusion chromatography (Fig. S9, 7.8 x 300 mm, Ultrahydrogel 250, Waters Corporation, Milford, MA), at a constant 1

mL/min flow rate using DI Water. (top) DI water alone showing characteristic solvent front (middle) Peptide calibration solution (Bruker Daltonics, Billerica, MA) defined in inset table with expected peaks labeled on chromatogram, demonstrating mass range and resolution of the SEC column and (bottom) GrBP5 solution showing one major peak in generally 1200-1400 mass region of the calibration solution. Minor peak exists as ~10% of total peak area while GrBP5 peak is quantified as ~90%, making up the majority of the solution.

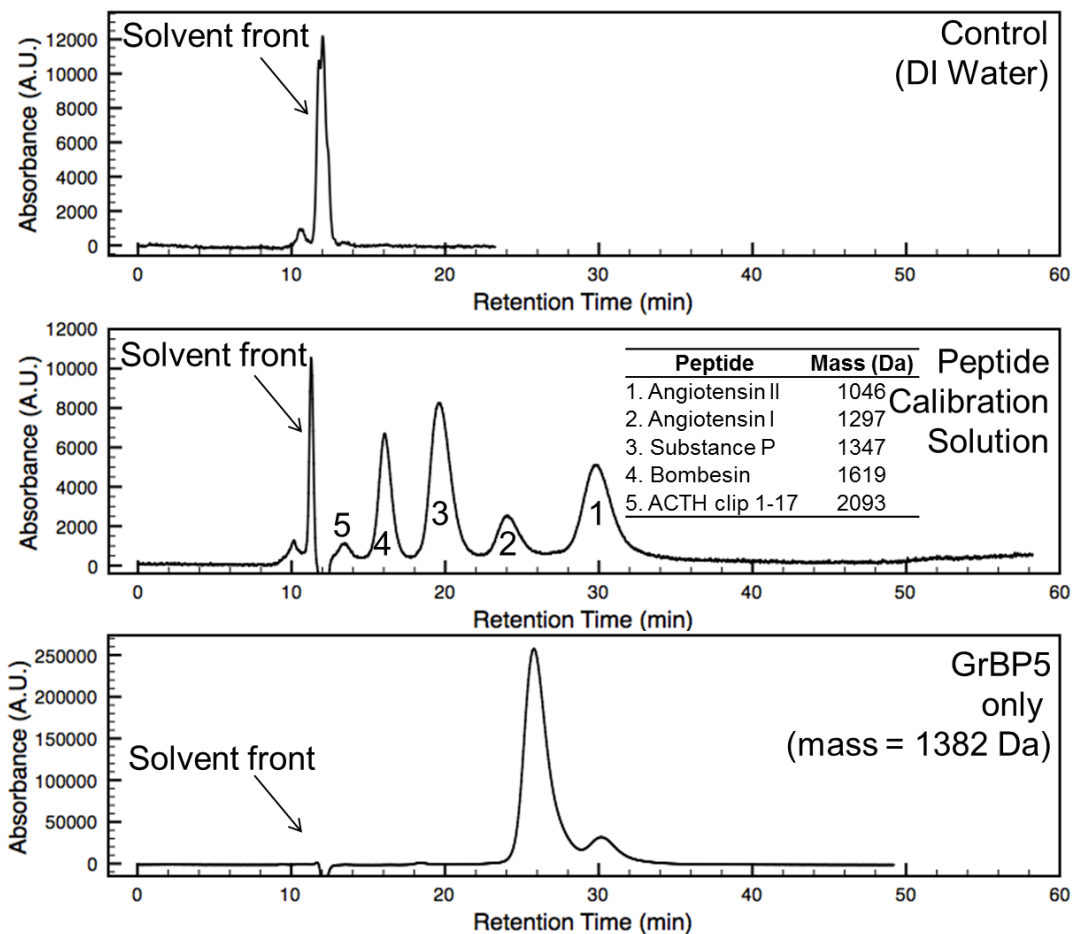
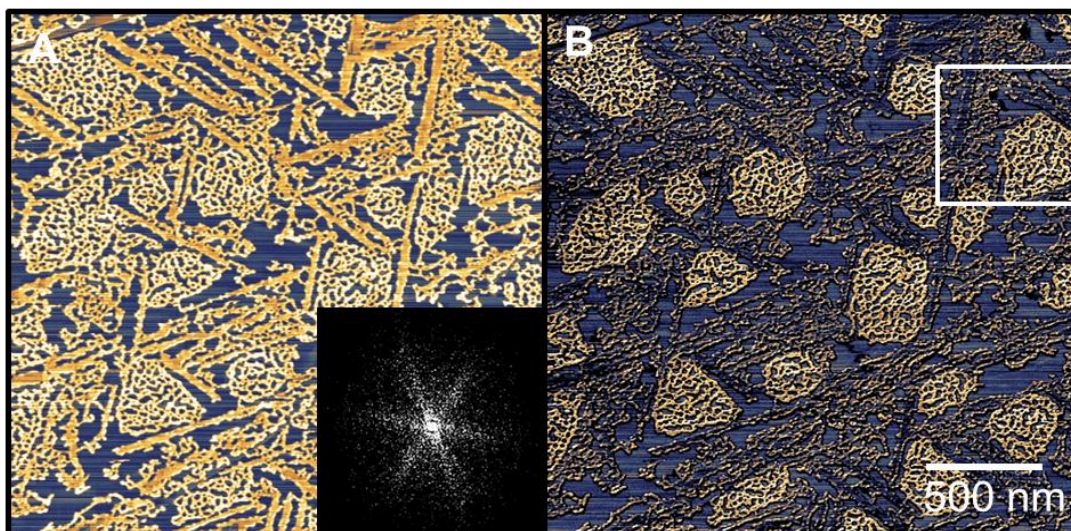
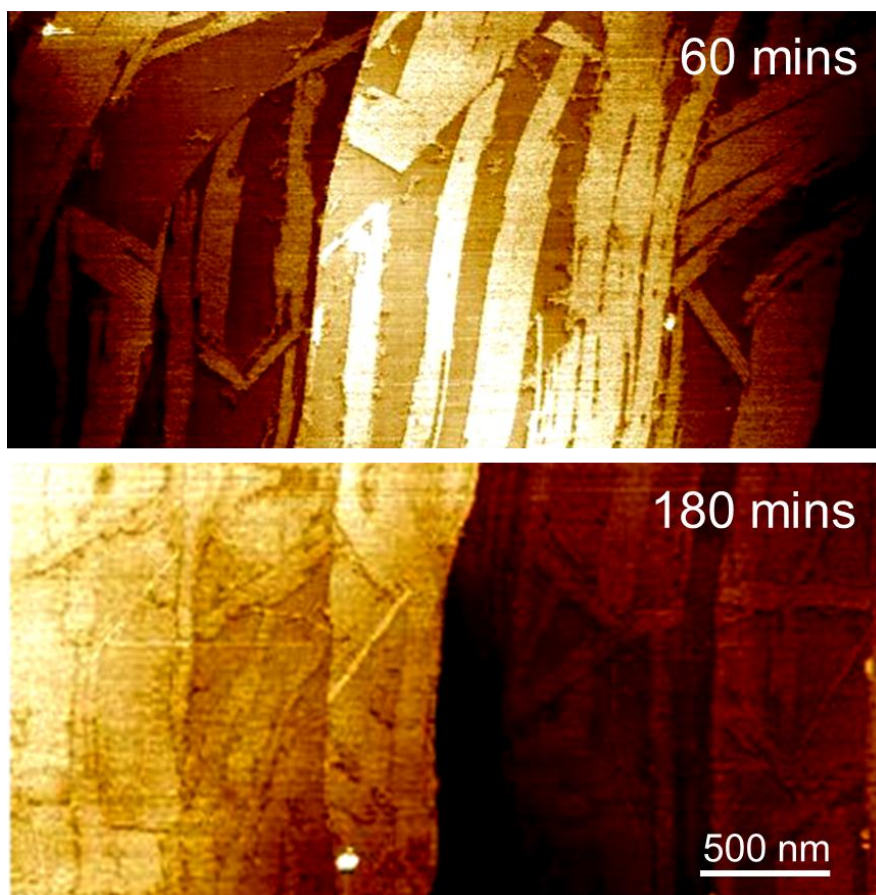


Figure S9. Size-exclusion chromatograms of DI Water, peptide standard solution, and GrBP5.

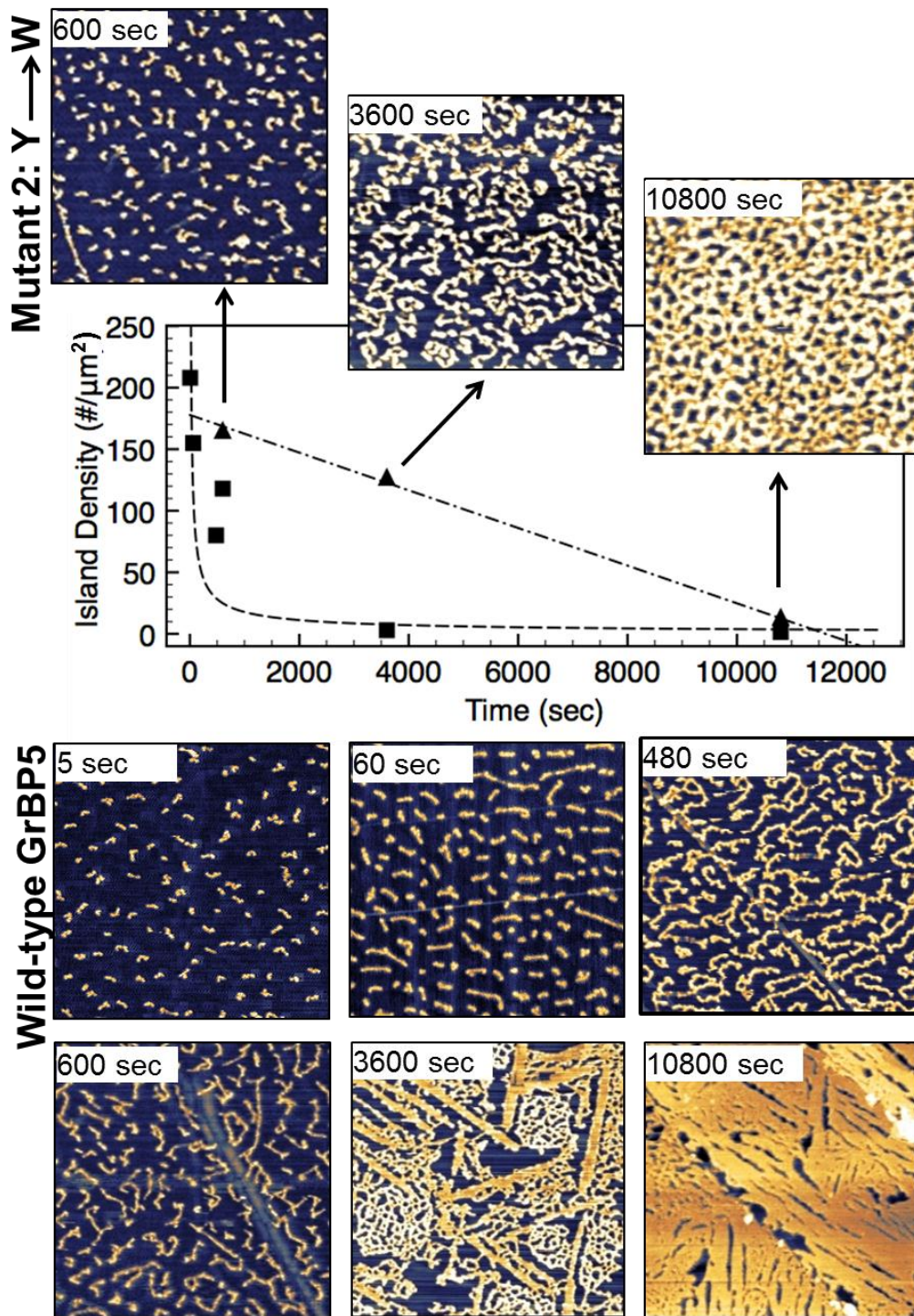
Supplementary Figures



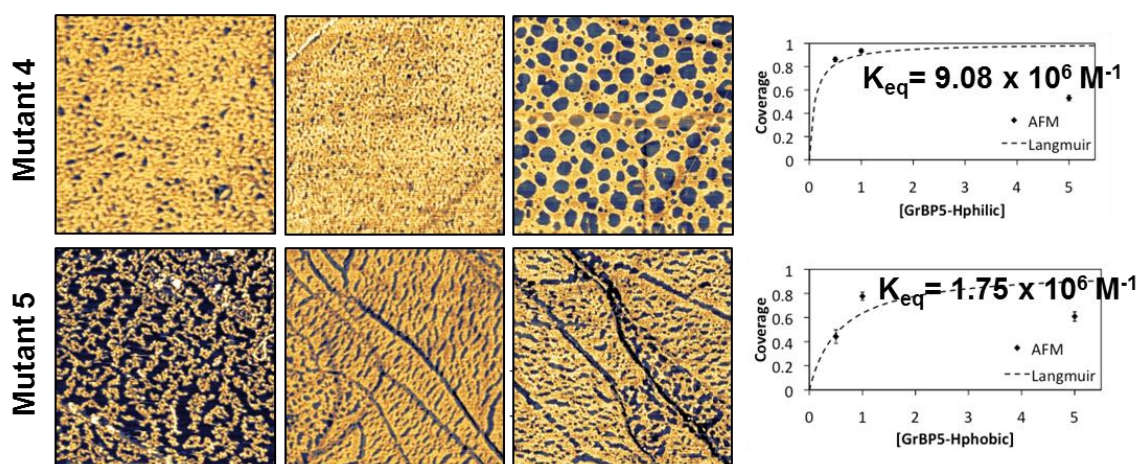
Supplementary Figure 1. Phase-lag AFM imaging of two-phases of GrBP5 on HOPG. (A) Topographic image of HOPG exposed to 1 μM GrBP5 for 1 hour, showing a clear interconnected ordered phase filled with an amorphous phase and FFT showing 6-fold symmetry of the ordered phase. (B) Phase-lag data from the same scan, showing large contrast between the bare graphite (blue) ordered phase (dark blue) and the disordered phase (yellow).



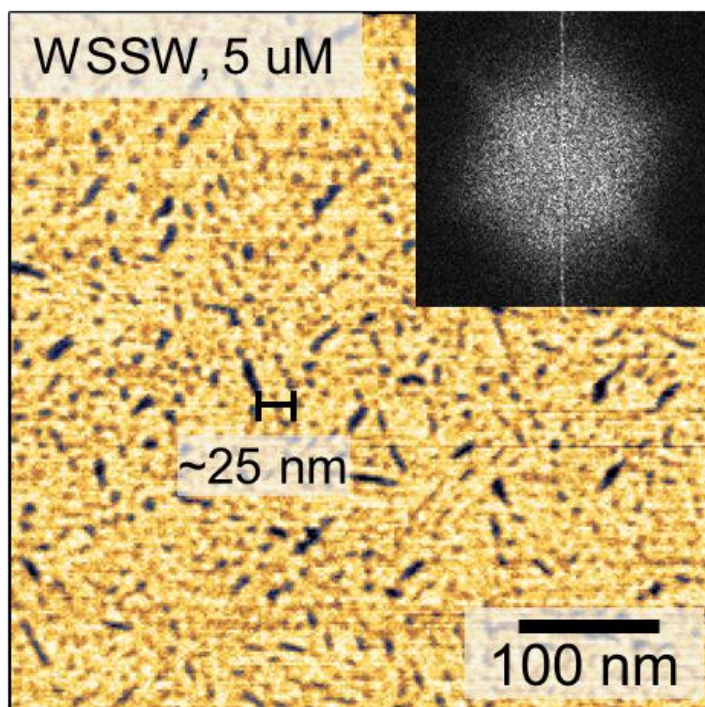
Supplementary Figure 2. Fluid-mode imaging of GrBP5 self-assembly on HOPG. 1 μM pre-mixed peptide solution was placed on graphite and scanned for 3 hrs with a Multimode (Bruker, Billerica, MA) AFM connected to a Nanoscope IIIa controller module using an indirect drive liquid-mode tip holder. Sharp Nitride Levers (SNL, 2-12 nm radius, ~ 0.6 N/m, Bruker, Billerica, MA) were used at 18 kHz resonance in DI Water. Tip dimensions are ~ 205 μm length x ~ 25 μm width.



Supplementary Figure 3. Quantification of island consumption, or coarsening rate, of WT-GrBP5 and Mutant 2 as shown in Fig 3 in the main text. While Mutant 2 coarsens slowly over 3 hrs, GrBP5 immediately forms a percolated state in ~900 secs. Time-lapse AFM images of Mutant 2 (top) and WT-GrBP5 (bottom) further show differences in surface mechanism. Early time adsorption studies (5, 60 and 480 sec) show first the growth of elongated islands and eventual percolation. All images are 1 μm x 1 μm in size.



Supplementary Figure 4. Characterization of GrBP5 and affinities of hydrophilic and hydrophobic mutants towards HOPG. Rows, top to bottom, are Mutant 4-Hydrophilic and Mutant 5-Hydrophobic at three concentrations exposed for 3 hours each. Columns, left to right, are surfaces exposed to 0.5, 1.0 and 5.0 μM peptide solution. Right-most column shows results of coverage quantification at the conditions shown and least-squares Langmuir fitting for K values displayed in each plot. All images are 1 μm x 1 μm in size.



Supplementary Figure 5. Zoomed in image from Supplementary Figure 5 of M2 at 5 uM showing very fine ordered structures ranging 10-30 nm in size. Structures are six-fold symmetric as observed by the inset FFT. Incubation was 3 hours.

References

1. S. Donatan, H. Yazici, H. Bermek, M. Sarikaya, C. Tamerler, M. Urgan, *Mat. Sci. and Eng. C*, **29**, 14 (2009).
2. M. Gungormus, H. Fong, I.W. Kim, J.S. Evans, C. Tamerler, M. Sarikaya, *Biomacromol.*, **9**, 966 (2008).
3. C.F. Barbas, D.R. Burton, J.K. Scott, G.J. Silverman, *Cold Spring Harbor Laboratory Press*, 2001.
4. I. Langmuir, *J. Am. Chem. Soc.*, **38**, 2221 (1917).